Satellite ocean colour based Harmful Algal Bloom identification for improved risk assessment and mitigation

Marié E. Smith[1*], Stewart Bernard[1]

[1]NRE-Earth Observation, CSIR, Rosebank, Cape Town, South Africa

[*]To whom correspondence should be addressed; E-mail: msmith2@csir.co.za

The aquaculture industry faces environmental threats from harmful algal blooms (HABs), which have the potential to cause devastating economic losses. Satellite earth observation offers a cost effective method for operational monitoring of HABs over vast areas. Whilst the Chl-a product, often used as a proxy for phytoplankton biomass, can be used to indicate high biomass blooms, there is a clear need for value-added products that not only alert on bloom presence, but also on the bloom type and persistence. The high biomass nature of the South African regional waters provide strong assemblage related spectral variability, which can be exploited with the spectral bands of OLCI and MERIS. This study demonstrates the identification of different phytoplankton types relevant to the aquaculture industry of South Africa. Thresholds of the reflectance peak in the red and NIR are related to phytoplankton count data, in order to identify blooms that pose a high hypoxia and/or toxicity risk. These techniques are applicable to both OLCI and MERIS reflectance data and are routinely used by the aquaculture industry in South Africa for timely risk assessment and mitigation. Application to both MERIS and OLCI not only ensures future monitoring capability, but also allows the creation of a historical risk climatology that can guide the site selection of industries sensitive to the presence of HABs, such as aquaculture farms and desalination plants.

1 Introduction

Aquaculture is a burgeoning industry in South Africa and plays a vital role in the country's blue economy. The marine aquaculture sector centers around mussel, oyster and abalone farming, with most facilities situated along the west coast in close proximity to the productive Benguela current upwelling system. However, the industry faces environmental threats from harmful algal blooms (HABs), with risk factors and mitigation strategies that differ for each sector. Whilst the herbivorous abalone are at risk of mechanical damage, paralysis, and anoxia, all primarily associated with dinoflagellate species, the filter-feeders (i.e. mussels and oysters) are more vulnerable to the accumulation of biotoxins produced by some dinoflagellates and the diatom *Pseudo-nitzschia*. Environmental and farm management requires near real-time information, not only on the presence of these blooms, but also the phytoplankton type, bloom proximity, spacial extent, and persistence to allow timely and informed decision making.

Ocean colour remote sensing provides a cost-effective and valuable tool in the detection and monitoring of various types of phytoplankton blooms (see references in (*1*)). The blue-green water-leaving reflectance signal generally dominates in open ocean environments, whilst this signal shifts to the red-NIR spectral region at Chlorophyll *a* concentrations ([Chl-a]) of approximately $>$15 mg m^{-3} (*2*). The optical environment off the west coast of South Africa can be described as phytoplankton dominated, with other constituents contributing relatively little to the water-leaving reflectance signal; however, the wide range in phytoplankton biomass requires adaptable remote sensing approaches that can utilize the most appropriate reflectance signal (*3*).

[Chl-a] is routinely derived from satellite reflectance, but does not provide direct information about inherent phytoplankton-related risk. This study aims to relate spectral features of water-leaving reflectance in the red-NIR directly to specific phytoplankton types of particular concern to the marine aquaculture industry of South Africa. We focus on application to reflectance data from the MEdium Resolition Imaging Spectrometer (MERIS) and the Ocean and Land Colour Imager (OLCI), as both sensors have good spectral covarage in the red-NIR region. The primary objective is to determine the presence and detection thresholds for waters dominated by either dinoflagellates or *Pseudo-nitzschia*.

2 Data and methods

In situ water samples were collected at a station in St Helena Bay approximately 4 km off of Lambert's bay (32.0845 ^{o}S 18.2691 ^{o}E) in late summer (between February and April) of 2004-2008. Chlorophyll *a* concentration was measured by fluorometric analysis (*4*) using 90% acetone with the use of a Turner Designs 10-AU Fluorometer according to accepted protocols (*5,6*).

Phytoplankton samples were taken at the surface, fixed in buffered formalin to a concentration of 0.5%, and counted using the Utermöhl method (*7*). In-water radiometric measurements were made with a hyperspectral Tethered Satlantic Radiometric Buoy (TSRB); further details on measurements, processing, and uncertainties can be found in (*3*).

Fuzzy c-mean clustering was performed on the *in situ* radiometric data (N=68) at wavelengths resampled to the MERIS/OLCI bands centered at 665, 681.25, 708.75 and 753.75 nm; two to nine clusters were tested. Principal component analysis (PCA) was performed on the same wavelengths, for both the entire dataset and individual clusters. The scores of the first three principal components (modes) of variance were use in correlation analysis to [Chl-a], reflectance peak height, and phytoplankton structure. Both PCA and clustering were only applied as exploratory data analysis tools, aimed at determining thresholds for classification purposes that correspond to changes in phytoplankton type dominance.

A line height algorithm, similar to the fluorescence line height (*8*), with a baseline formed by the water-leaving reflectance (ρ_w) between 665 and 753 nm was applied to all spectra, as demonstrated in equation 1; the peak heights at both 681 ($LH681$) and 709 nm ($LH709$) were calculated. The reflectance peak at 681 nm is generally associated with Chl-a fluorescence emission; however, at higher biomass this peak shifts to longer wavelengths due to the combined effects of increased phytoplankton absorption and backscattering, as well as pure water absorption. The maximum value of the two peak heights, as well as the line height ratio (LHR) of $LH709$ to $LH681$ (*9*), were used in the classification process.

$$LH(\lambda_{peak}) = \rho_w(\lambda_{peak}) - [1.005 \times (\rho_w(753) - \rho_w(665)) \times (\frac{\lambda_{peak} - 665}{753 - 665})] \quad (1)$$

Satellite data from the Ocean and Land Colour Imager (OLCI) on board Sentinel-3A (processing baseline 2.23; IPF version 06.11) were obtained from a ftp site (ftp://oda.eumetsat.int) for Sentinel 3 validation team members.

3 Results

The first three principal components accounted for 98.9 % of the total variance in the red-NIR of the remote sensing reflectance (R_{rs}) dataset (figure 1). The first mode showed a significant positive correlation to both peak height and [Chl-a], indicating that biomass drives the magnitude of the R_{rs} spectra in the red-NIR, while the percentage composition of diatoms and dinoflagellates had oposing effects on the spectral magnitude. Mode 2 indicated that increased [Chl-a] leads to a decrease in R_{rs} at 665 nm and an increase at 709 and 753 nm, associated with increasing phytoplankton absorption and backscattering, respectively. Mode 3 showed that the presence of *Pseudo-nitzschia* and dinoflagellates increases the fluorescence and 709 peaks, respectively.

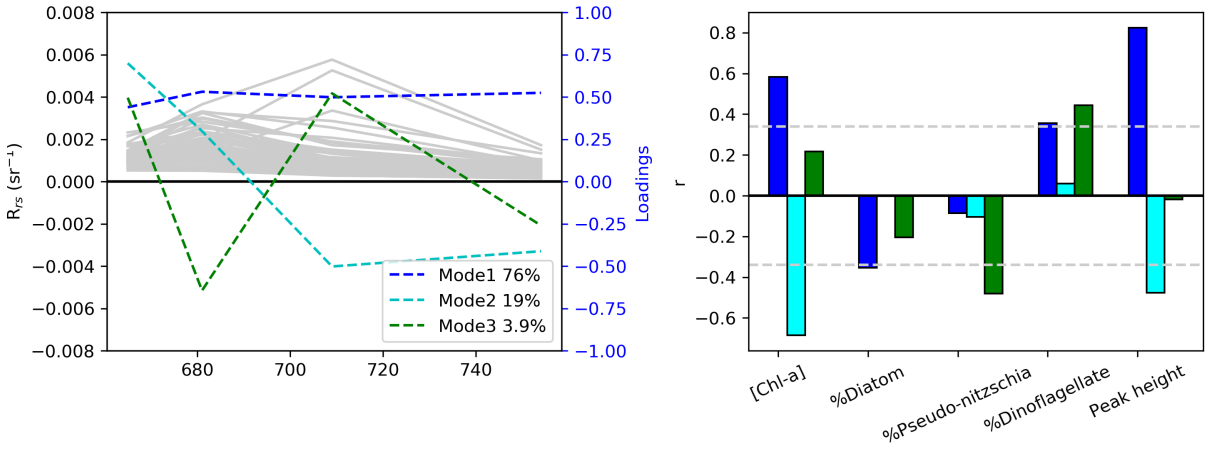

Figure 1: Results from the principal component analysis of the *in situ* reflectance between 665 and 754 nm (N=68). The coloured lines on the left show the loadings of the top three modes of variability in the reflectance dataset; the bars on the right show the correlation between these modes and key variables. Grey horizontal lines indicate the 95 % significance level.

FCM clustering resulted in five distinct and meaningful groupings of increasing peak heights and [Chl-a]. There is a great deal of ambiguity between clusters in terms of [Chl-a], particularly in the moderate to high biomass range (10-30 mg m^{-3}), as shown in figure 2b; however the peak height showed clearer discrimination between clusters. PCA of individual clusters revealed that only clusters three to five had any significant correlation to the variables (results not shown); thus only these three clusters were used to create the classification framework.

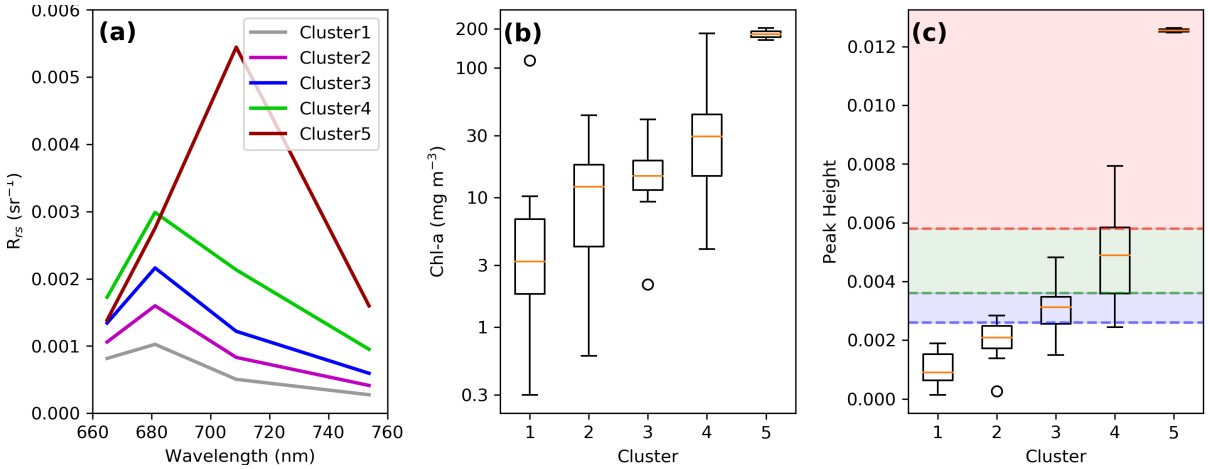

Figure 2: Mean cluster spectra (a), and boxplots of the [Chl-a] concentration (b) and peak heights (c) per cluster (Note: peak heights are provided for ρ_w).

Cluster 3 consists of moderate biomass of mixed assemblages, whereas cluster 5 was dominated by high biomass dinoflagellates. Cluster 4 represented a transition zone where the red shift occurs; within this cluster the LHR was a useful indicator of peak position and species composition. Waters dominated by *Pseudo-nitzschia* were distinguishable from other diatom blooms by a low LHR (below 0.3, indicating that $LH709$ was much smaller than $LH681$), whilst LHR$>$1 represented dinoflagellate-dominated waters; otherwise this cluster represented moderate to high biomass mixed assemblages (usually slightly diatom dominated).

The LHR, as well as the 25th and 75th percentiles of clusters three and four (indicated by the horizontal lines in figure 2c) were used as thresholds for a reflectance classification framework (shown in table 1) to indicate changes in phytoplankton type dominance and biomass.

Table 1: The classification framework for phytoplankton type dominance, based on thresholds of peak height and line height ratio (LHR).

Peak Height thresholds	**LHR$<$0.3**	**0.3$<$LHR$<$1**	**LHR$>$1**
$>$0.0026		mixed assemblage, moderate biomass	
$>$0.0036	*Pseudo-nitzschia* dominated	mixed assemblage, high biomass	dinoflagellate dominated, high biomass
$>$0.0058			dinoflagellate dominated, very high biomass

4 Discussion

At the relatively high concentration of biomass that regularly occurs in the southern Benguela, the largest spectral signal is often found in the red-NIR; under these high biomass conditions it is useful to avoid the blue-green spectral region, where the uncertainty resulting from aerosol extrapolation can be more extreme than in the red-NIR. The use of thresholds based on line height algorithms and ratios, instead of absolute reflectance values, also mitigates the potential spectral offsets and errors that might result from the atmospheric correction process.

This study represents a spectral classification scheme, applicable to both *in situ* and satellite reflectance, for the detection of phytoplankton types relevant to the aquaculture industry of South Africa. Although the classification is primarily qualitative, it is based on species-related optical signatures and count data, and provides more direct risk-related information for aquaculture management than traditional maps of [Chl-a]. The lack of significant correlation to any of the variables in clusters one and two indicates that the lower detection limit for this method of phytoplankton type identification is approximately 15 mgChl-a m^{-3}, which corresponds to

the shift in the spectral signal to the blue-green. At lower biomass levels the spectral features in the blue-green wavelengths would be more useful for detecting different phytoplankton types.

This classification scheme is applicable to OLCI sensors (example image shown in figure 3), ensuring utility of this classification technique for the next 20 years. It is also applicable to archive MERIS data and can be utilized to produce risk climatologies to guide future aquaculture and desalination site selection.

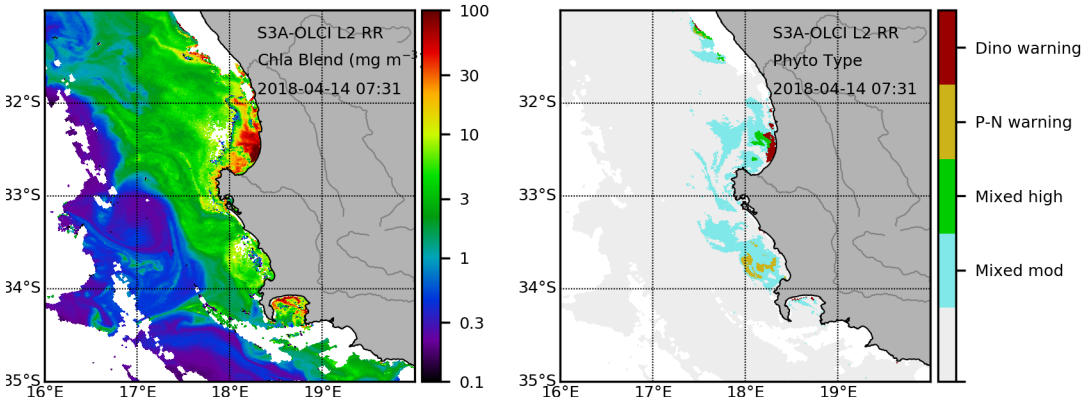

Figure 3: Satellite products derived from S3A-OLCI for the 14th of April 2018. The left panel shows [Chl-a], whilst the right panel shows the derived phytoplankton type classification; classes include dinoflagellate (red) and *Pseudo-nitzschia* (yellow) dominated waters, as well as high (green) and moderate (blue) biomass mixed assemblages.

It is important to note that the method presented here is not meant to be a species-level identification or to provide absolute counts and concentrations. Instead, it is merely a tool to identify optical features that correspond to phytoplankton that are associated with increased risk to aquaculture. The use of remote sensing for HAB monitoring is most powerful when informed by coincident *in situ* information such as phytoplankton counts and bio-optical buoys. Once a bloom has been identified as harmful, this classification method can aid in the detection, determining the spatial extent, trajectory, and possible intensification or dissipation of blooms, thus supporting the risk mitigation and decision making process at environmental management level and aquaculture facilities.

Acknowledgments

The authors wish to thank: EUMETSAT for funding to attend the Ocean Optics Conference, and for OLCI data; Grant Pitcher, Trevor Probyn, Andre du Randt from the Department of Agriculture, Forestry and Fisheries for *in situ* and phytoplankton count data.

References

1. D. Blondeau-Patissier, J. F. Gower, A. G. Dekker, S. R. Phinn, V. E. Brando, *Progress in Oceanography* **123**, 123 (2014).

2. L. Robertson Lain, S. Bernard, H. Evers-King, *Optics express* **22**, 16745 (2014).

3. M. E. Smith, L. R. Lain, S. Bernard, *Remote Sensing of Environment* **215**, 217 (2018).

4. O. Holm-Hansen, C. J. Lorenzen, R. W. Holmes, J. D. Strickland, *Journal du Conseil* **30**, 3 (1965).

5. J. Mueller, *et al.*, *NASA/TM-2003* pp. 15–26 (2003).

6. A. Knap, A. Michaels, A. Close, H. Ducklow, A. Dickson, *JGOFS, Reprint of the IOC Manuals and Guides No. 29, UNESCO 1994* **19** (1996).

7. R. Hasle, *Phytoplankton manual* pp. 88–96 (1978).

8. J. Gower, R. Doerffer, G. Borstad, *International Journal of Remote Sensing* **20**, 1771 (1999).

9. B. Tao, Z. Mao, D. Wang, J. Lu, H. Huang, *Remote Sensing of the Ocean, Sea Ice, Coastal Waters, and Large Water Regions 2011* (International Society for Optics and Photonics, 2011), vol. 8175, p. 81751K.